OVERVIEW OF USBM MICROSEISMIC INSTRUMENTATION AND RESEARCH FOR ROCK-BURST MITIGATION AT THE GALENA MINE, 1987-1993

By Louis H. Estey[1]

ABSTRACT

Mining-related microseismic activity at the Galena Mine, Wallace, ID, was targeted by the U.S. Bureau of Mines for studies of possible indicators of imminent rock bursts. Two systems were developed and deployed for microseismicity studies: one involving routine monitoring of several rock-burst-prone stopes and the other using digitally recorded signals. Research included a complete analysis of microseismic location errors for both systems. P-wave polarity patterns and focal mechanisms were correlated with local geology and intrastope activity. Evidence for sympathetic interstope activity was found. In a tomographic study, the area of greatest velocity decrease in a pillar that had been acoustically scanned did not correlate with microseismicity. A correlation was found between seismicity and sudden offsets in stope closure gage and borehole pressure cell signals, though aseismic creep accounted for 20 to 70 pct of the closure signals. Clustering, fractality, and planarity analyses were done on the microseismic data. Research at the Galena Mine indicates there is not a reliable indicator of all rock bursts that can be identified at the present time. For rock-burst forecasting, it may be crucial to identify, characterize, and measure the mechanics of mine geologic structures in both seismic and aseismic areas of a mine.

INTRODUCTION

A rock burst can be considered to be a seismic event in a hard-rock mine that caused damage to mine structure or caused or could have caused personal injury or death (Swanson and Sines, 1991). Rock bursts at the Galena Mine, Wallace, ID, have been occurring since the mid-1950's, when mining began at the 2400 level at depths of almost 1 km and deeper. This onset roughly coincided with mining operations moving from the softer St. Regis Formation down into the harder and more competent Revett Quartzite (Hobbs and others, 1965), which continues down to at least the 5500 level.

An overhand cut-and-fill method of mining has been used at the Galena Mine to remove ore from the nearly vertical, narrow (1- to 2-m wide) veins. Horizontal drifts in these veins were opened on levels every 60 m down to the 3400 level and every 90 m below that. Rock-burst problems often started when about three-quarters of the vertical extent of certain veins had been removed between the drifts of two consecutive levels, presumably coinciding with a critical geometry and/or stress state.

The sizes of rock bursts at the Galena Mine have been characterized using a local-magnitude (M_L) scale (Swanson and Sines, 1991), which is a cousin of the Richter-magnitude scale. The largest rock bursts at the Galena Mine have probably been about M_L 3.5, equivalent to moments of about 200,000 to 300,000 GN•m. The largest rock burst occurring between 1987 and 1993 was about M_L 3.1 (about 70,000 GN•m). The smallest damaging rock burst during this time was about M_L 0.5 (about 8 GN•m), and the smallest rock burst that could have caused personal injury or death was about M_L -0.5 (about

[1]Geophysicist, Denver Research Center, U.S. Bureau of Mines, Denver, CO.

0.2 GN•m). During the last few years, the rate of rock burst occurrence has been about one event of M_L 1 or greater per month (Swanson and Sines, 1991).

By event count, most seismic activity at the Galena Mine occurs as "microseismic" events, where a microseismic event can be considered to be any event smaller than about a local magnitude of 3 and having a practical detection lower limit of local magnitude of about -5.[2] This definition is consistent with the conventional understanding that a "seismic" event is large enough to be recorded and located using some portion of a regional or world-wide, array, such as the World-Wide Standard Seismologic Network, and that a seismic event currently has a practical detection lower limit of local magnitude of about 2.5 to 4.5 for these types of arrays (Engdahl and Rinehart, 1991). The largest rock bursts in the Coeur d'Alene district qualify as seismic events. Obviously, by these seismological quantitative measures, there is some overlap in magnitude between what is considered a rock burst and what is considered a large microseismic event or a small seismic event. In reality, perhaps the only distinction is happenstance: Whether a large microseismic event or a small seismic event happens to be located or oriented in such a way that it does or does not cause damage to mine structures and/or cause enough rock to be expelled into a mine opening to be hazardous. Therefore, in this paper a microseismic event is considered to be an event that is not a seismic event (i.e., not large enough to be detected on a wide-area or world-wide array) and is not a rock burst (i.e., no damage is done to mine structures and it is not considered to be hazardous).

The number of detectable microseismic events at the Galena Mine when the mine was in production was truly astounding, well in excess of 1 million per year. Some of the more active stopes generated many hundreds of thousands of microseismic events per year, of which 100,000 per year could be located by a routine monitoring system (described in the section on "Instrumentation" in this paper).

The two primary tenets that had been argued that would help solve the rock-burst problem were that (1) there should be anomalous microseismic activity before a rock burst or (2) there should be an increase in seismic velocity in the region that gives rise to the rock burst (Blake and others, 1974) due to some increase in stress. By the mid-1970's, the second idea was abandoned, and research was redirected toward obtaining direct stress measurements, rather than velocity surveys, in a burst-prone area (Leighton, 1976). However, this approach also did not prove useful because the observed changes in stress were coseismic (i.e., occurring at the same time as a microseismic or seismic event).

Microseismic events were still targeted for study as possible indicators of subsequent—and less frequent—rock-burst activity, due in part to the occurrence of microseismic events in large numbers. Other reasons were that microseismic events can be easily detected by sensors approximately in the acoustic range (Hz to kHz), and they can be detected passively, i.e., no intentional sources are needed. Also, the approach of studying small events to learn more about the characteristics of large events is exactly analogous to studying so-called foreshocks and aftershocks to learn more about large and moderate earthquakes.

This paper is an overview of U.S. Bureau of Mines (USBM) research performed at the Galena Mine from 1987 through mid-1993, done in cooperation with ASARCO, Inc., in an effort to reduce hazards associated with rock bursts. Much work done by the USBM and ASARCO at the Galena Mine precedes 1987 (Blake, 1971; Blake and others, 1974; Leighton, 1976; Leighton, 1982; Rowell and Yoder, 1984; Coughlin and Sines, 1985).[3] However, in recent years, USBM research has had a more distinct seismological emphasis. In late June 1992, the Galena Mine was placed on standby mode, essentially terminating USBM rock-burst research at the mine, but further monitoring of the decay of microseismic events—and a few rock bursts—continued until mid-1993. The analysis of these data continues.

INSTRUMENTATION

Two types of passive monitoring systems were developed and deployed at the Galena Mine. The first system is referred to as the routine monitoring system and the second is called the digital research system.

ROUTINE MONITORING SYSTEM

The routine monitoring system was developed for continuous monitoring of both microseismic and rock-burst activity in rock-burst-prone stopes, though such a system

[2]This is equivalent to a moment of 10 N•m, about 13 orders of magnitude smaller than the largest rock bursts that occur at the Galena Mine.

[3]Additional information from W. Blake and F. Leighton, USBM, 1961 and 1969.

could be used anywhere in the mine where microseismic activity occurred. For each monitored stope, this system consists of the following hardware units: (1) an array of high-frequency accelerometers, (2) 12-V preamplifiers, (3) four-conductor cables to (4) a rock-burst monitoring unit built by Science Applications International Corp. (SAIC), of Las Vegas, NV, installed at or near the stope, (5) RS-232 cables to 6) an Apollo workstation located in an underground instrumentation room. The accelerometer stations were always uniaxial; the one component usually measured the near-horizontal component of ground acceleration at a rib-mounted sensor position (station).

The design of the SAIC unit was based on a portable microseismic recorder developed and tested earlier by the USBM (Coughlin and Sines, 1985). Each SAIC unit was designed to provide stable, 12-V power to the preamplifiers near each accelerometer, digitally analyze up to 16 incoming signals from the accelerometer array, decide when a transient event occurs on five or more channels, select relative arrival times for all channels possible via a floating-threshold, first-break algorithm to the nearest 0.1 ms, and provide a measure of the energy by time integration of the square of the voltage signal over a fixed time window on up to four preselected channels.

For each transient event that triggers the SAIC unit, the internal time of the SAIC unit, the relative arrival times for each channel, and the energy measures are transmitted via the RS-232 cables back to a dedicated workstation for the particular array. An array file in the workstation holds the coordinates of the accelerometers of the array; this file is updated manually when the actual sensor array is changed. As event information from the SAIC unit is read by the workstation, software screens arrival times, locates the event if possible, and displays the event location on the workstation monitor using three orthogonal views of the stope. In addition, the raw data from the SAIC unit are stored in one file on the workstation system (the times file) and the processed location is stored in another file (the location file). The total amount of time from detection of an event by the SAIC unit to display of the event location at the workstation and resetting the SAIC unit is about 0.3 s, thus providing near-real-time monitoring of stope microseismic activity.

The routine monitoring system was an outgrowth of earlier systems developed for and tested with a single stope array. The complete routine monitoring system, however, links several SAIC-Apollo systems together with a token ring local area network (LAN) at the underground instrumentation room, allowing data archiving and other system activities from any single workstation node on the LAN (Steblay and others, 1990a, 1990b).

This arrangement allowed the system at the Galena Mine to be expanded so that ultimately 8 arrays, composed of up to 128 accelerometers, were monitoring up to 11 rock-burst-prone veins in production throughout the mine. In addition, almost 3 km of six-conductor, fiber-optic cable was installed from the office-dry building on the surface, along the surface adit to the No. 3 shaft, down the No. 3 shaft to the 4600 level, and about half a kilometer along the 4600 level to the underground instrumentation room. Using optical transceivers and two of the fiber-optic lines allowed a separate workstation on the surface to be included in the token ring LAN, and thus data from any instrumented stope could be easily accessed at the surface in near real time. Data for all monitored stopes (array files, times files, and location files) were written to cartridge tape and mailed back to the Denver Research Center (DRC) for further processing. Monitoring and event detection continued in three to four stopes through at least September 1994, 27 months after the initiation of standby mode at the Galena Mine.

The near-real-time display (microseismic event location in relationship to stope geometry) possible with this type of system proved to be a valuable tool for mine personnel. However, from a geophysical research point of view, any analyses are limited in scope if they involve temporal and/or spatial characteristics of event locations or crude estimates of event energy. For example, some of the fundamental pieces of seismological data missing for each event are the identity of the first-break point, the polarity of each incoming wave at each sensor, estimates of later arrivals (such as any S-wave arrivals), and so on.

DIGITAL RESEARCH SYSTEM

To overcome some of these limitations, a second type of system, called the digital research system, was developed, primarily for geophysical research (Swanson and Boler, 1988a; Boler and Swanson, 1990). The first use of this system took advantage of hardware already in place for the routine monitoring system. The SAIC unit was still used to power the accelerometer preamplifiers. The analog signals from the sensors continued to be input to the routine monitoring system as before, but these analog signals were also input into the second system in which the signals from each event above a certain threshold were digitized and recorded.

Satisfying several simultaneous requirements led to the creation of a data acquisition system combining modular computer-automated measurement and control (CAMAC) instruments with a UNIX-based workstation. CAMAC modules for amplification, analog-to-digital (A/D) conversion, memory, and CAMAC crate control are manufactured by a number of companies. Furthermore, as the research needs of the system evolved, different CAMAC modules were added without the necessity of redesigning the basic hardware of the system, and software modifications to the workstation were minimal. It should be

recognized that the digital research system was not designed to replace the routine monitoring system, but to collect highly detailed "snapshots" of microseismic activity that would be amenable to detailed analysis of each recorded event (Swanson and Boler, 1988b). This system was used to collect microseismic data centered on the 4300 level during production in the 120 vein around the 115 stope for 4 months in 1988, during production and destressing in the nearby 104 vein around the 99 stope from August 1989 through March 1991, and finally to collect about a month's worth of data in each of five stopes from October 1992 through April 1993.

The flexible characteristics of the digital research system eventually allowed simultaneous monitoring of accelerator signals of kilohertz frequencies and quasistatic rock mechanics measurements in the 99 stope. The former requires monitoring and high-density digitizing of transient signals that can occur at any time, and the latter requires only periodic point sampling of each pertinent channel. A second system was added later for a lower frequency underground mine-wide array using velocity geophones of 3 to 250 Hz. Furthermore, for both systems, as many stations as possible were triaxial (three mutually perpendicular uniaxial sensors installed to measure all components of ground motion at a single station). Our goal by 1991 was to monitor large events throughout the mine with a mine-wide array of eight underground triaxial stations and a dedicated CAMAC-workstation system, and to continue to monitor microseismic activity with another CAMAC-workstation system in various stopes that were rock-burst prone.

The digital research system tends to be limited by the hard disk due to the large size of the binary data files of the digital waveforms. The data files for a single microseismic event are often on the order of 0.1 to 1 Mbyte in size (e.g., 32 channels with a sampling rate of 50 kHz, a time window of 0.1 s, and a dynamic range of 16 bits (2 bytes) per channel yields 0.32-Mbyte data files per event). During operation at the Galena Mine, limitations in technology, economy, and practicality allowed only about 200 to 300 Mbyte of free hard disk space for data. For some of the more active stopes, this disk-size limitation allowed only a few days of data collection before the hard disk would become full, requiring a tape dump and removal of files from the hard disk.

Finally, another set of optical transceivers were used with two more of the fiber-optic lines to the surface to establish a carrier-sense, multiple access with collision detection (CSMA/CD) LAN between the underground data acquisition workstation of the digital research system and another UNIX workstation at the surface. A pair of high-speed Telebit WorldBlazer modems allowed connection and high-speed data transfer over ordinary, nondedicated voice telephone lines. These modems have a built-in optimization for UNIX-to-UNIX copy (UUCP) protocol. Using a 19.2-kbaud RS-232 cable connection to the workstation and this protocol, transfer rates of almost 0.1 Mbyte of binary data per minute (1,600 bytes per second) are possible. Thus, data files for a few critical events could be copied from the underground digital research system to a workstation at DRC in a matter of minutes without stopping data acquisition.

SURFACE SEISMIC SYSTEM

By late 1990, we realized the scientific and practical utility of also establishing a surface array and decided to experiment with another type of digital research system. This second digital system is the PCQuake system of the International Association of Seismology and Physics of the Earth's Interior (IASPEI), which had just become widely available (Lee and others, 1988; Lee, 1989). Being based on a personal computer (PC), it is inexpensive compared to a CAMAC-workstation system.

The basic PCQuake system is a dedicated PC that monitors up to 16 A/D channels, each with 12-bit dynamic range. This allows monitoring of five triaxial stations with one free channel. In addition, the PC clock can be forced to Coordinated Universal Time (UTC) (plus or minus an integer number of hours) using the Inter-Range Instrumentation Group (IRIG) B time code input to a TrueTime Model PC-SG synchronized generator card, which is installed on the PC bus. The IRIG-B code was supplied by a TrueTime Model 468-DC clock, which has an accuracy of ±0.5 ms when it is locked on to one or more of the Geostationary Operational Environmental Satellites (GOES).[4] By the time the Galena Mine was placed in standby mode, two triaxial stations and a few uniaxial stations were in place and linked to the surface PCQuake system by cable, using largely the same type of velocity sensors being installed with the underground mine-wide digital array.

ROCK MECHANICS

At the end of July 1989, an array of borehole pressure cells (BPC's) was also installed at one corner of a pillar formed by the 104-vein drift and the crosscut intersection on the 4300 level (Boler and Swanson, 1993a; 1993b). The purpose of this array was to monitor stress changes associated with seismic events (whether rock bursts or not) and planned destress blasts in the vein below the drift.

Each BPC is essentially an oblong, flattened, stainless-steel bladder encased in grout and sized so that it can be inserted into a standard borehole. After insertion into a

[4]The GOES system transmits a time code referenced to UTC which, when fully corrected, usually has an accuracy of ±0.10 ms.

borehole, the BPC is hydraulically pressurized to a level approximating a local maximum principal stress, and thereafter the hydraulic fluid pressure is monitored (Haramy and Kneisley, 1991) for example, using a Bourns 35-MPa pressure transducer.

The installed array consisted of three mutually perpendicular boreholes and eight BPC's oriented so as to be at maximum sensitivity to the three suspected principal directions of the local stress field. Two of the BPC's provided some redundancy. Logging of the pressure readings by CAMAC digital voltmeter on the digital research system began in February 1990. Readings were taken on every cell every 10 min and continued through March 1991.

In the 99 stope beneath the 104-vein drift on the 4300 level, a small array of three stope convergence gages was installed by June 1990 and was monitored through March 1991 (Boler and Swanson, 1992). These gages were designed to be inexpensive and expendable, but they had to be watertight and robust enough to withstand both the water-sand slurry used to backfill stopes and the production blasts as the stope was excavated upward in the ore vein. Internally, each gage consisted of a constant-tension spring motor that turned the wiper of a potentiometer. The voltage across this potentiometer in each gage was amplified and cabled back to the digital research system, which took a voltage reading on every gage every 10 min. The bidirectional gages were designed to measure only on-axis displacements and had a total range of 0.6 m. The limiting component for repeatable accuracy was the internal spacing of potentiometer windings, which limited the convergence steps and bidirectional reproducibility of the gage to 0.2 mm.

SOFTWARE

TIME-SYNCING

The final goal in seismological data collection at the Galena Mine was to coordinate digital waveform acquisition from a stope-level CAMAC-workstation system, the underground mine-wide CAMAC-workstation system, the surface PCQuake system, and two regional arrays [the North Idaho Seismic Network (NISN) (Lourence and others, 1993) and the Montana seismograph network (Stickney, 1993)] for monitoring rock-burst events and large microseismic events in the near and far fields. Although this final goal was not realized, it is noteworthy to understand why we were concerned with obtaining a common time base for all these arrays.

The P-wave velocity for the quartzites in the Silver Valley is roughly 5 km/s. Thus, if the NISN, the Montana network, and the local PCQuake system are each tied to a common time base (e.g., UTC) that has an accuracy of ±0.5 ms, this time uncertainty equates to an equivalent spatial drift and jitter of up to ±10 m in array coordinates when tying the data sets together, which is about equivalent to the accuracy of an inexpensive GPS survey of array coordinates. In other words, no significant additional errors would be introduced into a seismological inversion, such as event location, because of clock errors in the separate systems.

However, in tying a surface system to an underground system separated by 1.5 to 2 km, for example, this same ±10 m could be significant, because this would be equivalent to about ±10 m of random errors in array coordinates between the two systems for different events. We felt that if any local time base uncertainty between any surface system and any underground system could be reduced by an order of magnitude (i.e., an equivalent spatial jitter of about ±1 m), the result would be acceptable. Software experiments performed at DRC on a CSMA/CD LAN showed that probably the best that two UNIX workstation system clocks could be synchronized would be about ±1 ms owing to the nondeterministic nature of CSMA/CD packet traffic. Also, because of clock stabilities of only a few parts in a million, even if the two workstation clocks could be synchronized exactly at some instant, the clocks could drift apart in time by as much as a millisecond in only a few minutes.

Through further software experiments on the LAN at DRC, we determined that the clock drift of two separate workstations probably could be monitored to a precision of a few tens of microseconds, which is well within the synchronization target of 0.1 ms. Although the same experiments were never performed on the fiber-optic LAN at the Galena Mine, this precision probably could have been achieved there as well.

DATA ACQUISITION

The data acquisition and display software for the routine monitoring system is very tightly bound to the Domain-Aegis operating system and display manager of Apollo workstations. This attribute alone would make it very difficult to port to another type of computer. However, all the source code is written in C, and it should be possible to extract the functionality of many algorithms for use elsewhere.

Data acquisition by any CAMAC-based system will necessarily be tied to the type of bus selected for communication between the CAMAC crate and the controlling

computer. For the digital research system, a general-purpose interface bus (GPIB) crate controller was selected. Also, the Hewlett-Packard (HP) UNIX workstations selected as the controlling computer had a compatible HP interface bus (HPIB), HPIB being the forerunner of the GPIB standard. The data acquisition software developed for the research system is written in C and uses a small number of low-level HPIB function calls to communicate with the CAMAC crate.

Two different A/D systems were developed using CAMAC technology. One system involved use of modules built by DSP Technology, Inc., of Fremont, CA, resulting in a system with up to 100-kHz sampling and 12-bit dynamic range (Boler and Swanson, 1990). Because of the 12-bit resolution of the A/D modules, analog data for each channel were sometimes digitally recorded twice, once at high gain to capture the smallest events and simultaneously at low gain to avoid digital clipping of the larger microseismic events. This C software eventually evolved into the USBM's current in-house *TraqAcq* code.

The other system involved the use of modules built by KineticSystems Corp., of Lockport, IL, resulting in a system with up to 85-kHz sampling (with 16 channels) and 16-bit dynamic range. The KineticSystem A/D modules can be easily linked to provide a system that simultaneously captures up to 64 channels. We were able modify and test the original *TraqAcq* code to handle the KineticSystems modules with DSP amplifier modules in just 4 days, an accomplishment that demonstrates the flexibility of the data acquisition software design. This code is called *KS16Acq*.

For both sets of modules and their associated software, a standard HPIB interface is used between the CAMAC crate and the workstation. The total amount of time from triggering the digitizers on the CAMAC, to data transfer to the workstation, to setting up for the next triggering of the digitizers is proportional to the total amount of digital data saved for an event. This delay is about 16 s/Mbyte for both.

Both *TraqAcq* and *KS16Acq* are designed to work in a UNIX operating system and communicate with the CAMAC crate with GPIB commands. Both functions can also access a set of other UNIX commands that, for example, can be a sequence of event-processing filters to be applied to each event file recorded. This set of commands could pass the file on for first-arrival picking, event location, and archiving of the event location. A log of data acquisition startup, stoppage, warnings, and errors can be dumped to a log file or dumped to a printer. For field use, a simplified, menu-driven interface called *CamAcq* was written to start and stop either *TraqAcq* or *KS16Acq*, copy files from hard disk to tape, remove files from hard disk, plot event files, and do a variety of other tasks.

WAVEFORM MANIPULATION

Two graphical user interface (GUI) C programs were developed to manipulate the collected waveform files. One of these programs, *plot*, was based on HP's Starbase graphics functions and was simplified for field use to allow a minimum of functionality, which currently includes arbitrary record selection, waveform magnification, arrival picking, and event location with display of calculated arrivals. The other program, *sgp* (seismic graphics program), was modified after a version supplied by Lamont-Doherty Geological Observatory of Columbia University, New York, NY. This second GUI is for use in an X11 Window System environment. It currently includes all the functionality of *plot*, plus the capability of display or manipulation of waveforms in time domain or frequency domain, time-domain hodogram display for biaxial or triaxial sensor stations, focal-sphere first-motion display with interactive or software-search solutions, and other functionalities.

Another important set of C software adapted from Lamont-Doherty was that of UNIX filters for the waveform files. These filters currently include methods of forward and inverse fast-Fourier transforms, time-series signal inversion, detrending, demeaning, windowing, Butterworth filtering, P-wave arrival picking, attenuation correction, fast-Fourier transform integration and differentiation, event location in homogeneous or plane-layered media, source parameter fitting, and other functionalities. These filters, along with the two GUI waveform display programs, provide the backbone for analyzing the bulk of the digital waveform data collected by the digital research system.

THREE-DIMENSIONAL SOLIDS RENDERING

Another software tool was developed to display graphically the varied and complex three-dimensional assortment of data needed for tracking microseismicity in a mine. This assortment includes the microseismic locations themselves, mine openings, local geology, and calculated quantities such as three-dimensional stress or strain fields. Many of these items can vary as a function of time. An interactive graphics package, *4d_render*, which also uses HP's Starbase graphics functions, was developed to meet these needs. The additional use of HP's graphics hardware accelerators allows the calculation and display of realistic three-dimensional images (i.e., solids rendering) in near real time. Limited only by the amount of computer

memory, *4d_render* stores and links together in memory the data for an arbitrary number of graphics primitives, which are then accessed in an optimized fashion during the rendering. Taking advantage of many of the advanced features of Starbase, *4d_render* includes functionalities such as the specification of an arbitrary set of lighting conditions, solid or wire-frame surfaces, partial transparency of surfaces, arbitrary positioning of the viewer and image reference points, forward or reverse time-sequence display, and, when used in an X11 environment, a stereographic image pair. These and numerous other features of *4d_render* have made it an invaluable tool for combining and visualizing the diverse data sets and results used in research.

TEMPORAL AND SPATIAL STATISTICAL ANALYSES

Several new and innovative methods of statistical analysis were applied to the data collected by the routine monitoring system to discern temporal and spatial patterns of microseismicity (Coughlin and Kranz, 1991; Kranz and others, 1994).[5] These methods include fractal analyses of time of occurrence and locations of microseismicity, event attribute clustering, and planarity searches of spatial distributions of microseismicity. In addition, the decay of microseismicity following production blasts and rock bursts around the 99 stope was analyzed using the maximum-likelihood method of Ogata (1983) to determine modified-Omori decay fits.

RESEARCH RESULTS

EVENT LOCATION ERRORS

One of the first areas of research was an evaluation of event location errors that could be reliably associated with the locations produced by the routine monitoring system and by the digital research system (Swanson and others, 1992a, 1992b). The two systems must be examined separately because there are several major differences in the sources of error in the two systems.

The first source of error is the uncertainty in the coordinates of the sensor stations. For the routine monitoring system, station coordinates were estimated from using tape measures and mine maps. For the digital research system, in the worst cases, coordinates were obtained in the same way, and in the best cases, coordinates were surveyed. Using an electronic distance-measuring device on a theodolite, such a survey produced coordinates with uncertainties we estimated to be about ±5 cm. Performing a least squares fit between coordinates obtained with these two methods showed that the tape measure and mine map method results in an average error of about 1 m, and that an individual error for a single station, even in the horizontal direction, can be 2 m or more. Some portion of this error was probably attributable to changes in actual mine geometry due to large-scale deformation of the mine occurring between the time when the mine was originally surveyed and mapped and the time of the microseismic array installation, about 25 years for the 4300 level. From various surveys performed to obtain station coordinates, the magnitude of this deformation is estimated to be 0.2 to 0.4 m over distances of 100 m in crosscuts between veins and about 1 m or more in drifts on the levels.

The second source of error is the uncertainty in arrival time picks of the seismic ground motion at each sensor. For the routine monitoring system, the picks are accomplished in near real time by a hardware algorithm in the SAIC units. For the digital research system, the picks are done manually using one of the GUI's. In comparing differences in arrival time picks between the two systems of the same event, it was noticed that a hardware pick tended to be either coincident with or later than the corresponding manual pick. Differences in a suite of arrivals for different events showed that this delay of the hardware picking had a distribution that approximated an exponential function with a 140-μs time constant, and delays in excess of 1 ms are possible. With a P-wave velocity of about 5 km/s, this distribution is equivalent to distance errors from a few tenths of a meter up to at least 5 m on occasion.

The third source of error is in essence the same for both systems, i.e., the uncertainty in the velocity model used. The velocity structure in the vicinity of a stope is quite complex, owing to the volume of fractured rock and sand- and air-filled openings, as well as preexisting variations in local geologic structure. The velocity structure is in fact so complex and varies as a function of time in such a way that the only reasonable assumption that can be made is that some mean P- and S-wave velocities apply, though this assumption is obviously incorrect in detail. For the routine monitoring system, a mean P-wave velocity of 5.64 km/s had been previously determined on the basis of a set of test blasts involving sensors installed underground over a wide portion of the mine. In January 1990, another set of test blasts was done using the digital research system around the 115 stope; a mean P-wave velocity of 5.02 km/s was found with extremes of 3.26 and 5.70 km/s. For this test area, the slowest path was entirely near the stope, and the fastest path was through largely

[5]Kranz, R. L., J. Coughlin, and S. Billington. Characterization of Blasting and Rock Burst Aftershock Sequences in a Hard Rock Mine. Abstract in Workshop on Induced Seismicity (33rd U.S. Symp. Rock Mech., Santa Fe, NM, June 8-10, 1992). 1992, p. 11.

undisturbed country rock (Estey and others, 1990). It was also found that the country rock may be weakly anisotropic, but this finding was not explored further.

The fourth source of error involves the choice of location algorithm. The location algorithm used with the routine monitoring system was that of Blake and others (1974). For the digital research system, a variety of location algorithms were investigated, which included examining different basis functions (Swanson and others, 1992a) and solving the resulting system of equations using different L2-norm minimization (least squares) algorithms and an L1-norm minimization simplex method (Riefenberg, 1989a, 1989b). As a result of this investigation, it was discovered that the accuracy of a particular algorithm is strongly dependent on the types of errors in the total solution model, i.e., arrival times, station coordinates, and velocity model (Estey, 1990). In short, if all the sources of error are random, algorithms involving iterative gradient solutions tend to yield locations with the smallest spatial errors. These algorithms also tend to minimize the travel-time residuals of the location solutions. However, in the presence of a systematic error in the velocity, the algebraic algorithm and exact choice of basis functions used by Godson and others (1980) yield the smallest spatial errors, even though the gradient algorithms continue to produce location solutions with the lowest travel-time residuals. The algebraic algorithm of Blake and others (1974) tends to give poor results in either case. Because it was noted that the method described by Godson and others also does fairly well with the random error cases, and because the uncertainty in velocity seems to be one of the major contributors to final location errors, this location method was selected as the primary one for the digital research system.

The total amounts of spatial location errors were estimated by using synthetic numerical models incorporating the above errors and by locating actual test blasts in the 115 stope with a sensor array about 150 m in dimension. Average random location errors of ±0.7 m for the digital research system and ±3.6 m for the routine monitoring system occurred over large areas of the array, these average random location errors being dominated by the errors in arrival-time picking for both cases. An additional average location error component of ±1.2 m for the digital research system and ±7.0 m for the routine monitoring system occurs because of the choice of mean velocity and location algorithm. All of these errors are well modeled. However, based on the test blasts, an additional systematic location error of up to 10 m for locations within the array can occur for both systems, apparently resulting from additional uncertainty and variation in the velocity structure. Put another way, the random location errors for the routine monitoring system were found to be about five times larger than the best that can be achieved with the digital research system, but a velocity-based systematic error is about the same for both systems.

P-WAVE POLARITY PATTERNS

When the digital research system was first installed, one of the first areas of investigation was to see if information about the change of stress in a stope could be inferred from first-motion P-wave polarity data. Digital data from a 1-week production period in April 1988 were collected for about 250 locatable events using the 115 stope array of 11 uniaxial sensors. P-wave polarities were manually picked for these events. Various unknowns at the time precluded the use of traditional focal sphere methods for analyzing the P-wave polarities. Therefore, a pattern recognition search was performed to identify groups of events with consistent patterns of P-wave first motions as they had been recorded at the sensors. Six groups (a total of 54 events) were identified on the basis of the pattern recognition search, spatial relationships, and elimination of ambiguous polarities at one station.

This study (Boler and others, 1988; Billington and others, 1990a) clearly indicated that groups of microseismic events with similar P-wave polarity patterns existed and were identifiable. Also, it was found that there was a progression from one group of events to another in the rock mass surrounding the stope during the hours following routine production blasting. This observation of the migration of microseismic activity and its associated change in polarity pattern with event location is consistent with a transfer of stress around a stope following blasting and can be identified at the scale of only a few meters.

P-WAVE FOCAL MECHANISMS

A focal mechanism is a standard seismological method of projecting information received at an array of sensors back to a small imaginary sphere surrounding the source, or focal, region. The simplest focal mechanism to construct is that of the P-wave first motion, because P-waves are the fastest waves in a solid medium and are less likely to be contaminated by the coda of later waves received at a sensor. It is best to have triaxial sensor stations, especially when the P-wave energy will be arriving from an arbitrary direction, such as occurs when the stations are underground. However, with the routine monitoring system arrays, the data sets are dominated by uniaxial stations. These sensors are often mounted (for convenience) such that motion in the horizontal (or near horizontal) direction is best detected. This sometimes precludes use of polarity data from certain uniaxial stations, depending on the orientations of the ray paths from the source to the sensors and the uniaxial orientation of those sensors, because the sensors are insensitive to P-wave motion arriving in a direction normal to the axis of the sensor.

Seismic sources can usually be represented by slip on a fault surface (i.e., a shear dislocation), which gives rise to a quadrupole radiation pattern for both P- and S-waves

(Aki and Richards, 1980). For an elastically uniform, isotropic source site, the quadrupole has a symmetry center such that any point on the focal sphere can be projected through the center to the other side. Thus, only one hemisphere of the focal sphere needs to be considered. Also, nodal planes of zero P-wave motion occur in the plane of slip and on an auxiliary plane normal to the direction of slip.

Focal mechanisms were computed for several rock bursts and the microseismicity around them using the data collected by the digital research system (Boler and Swanson, 1993a, 1993b). Several important findings are that (1) focal mechanisms are found that are consistent with a quadrupole radiation pattern, implying slip on a locally planar surface, (2) the quadrupole quadrants are consistent with an elastically uniform isotropic or near-isotropic source region, (3) the orientation of one of the nodal planes of the focal mechanisms is in agreement with the local orientation of bedding plane faults in the mine, which strike about N. 45° W. and have near-vertical dips, and (4) composite focal mechanisms (i.e., superposition of data from more than one event on a single focal sphere) show that groups of events can have essentially the same source mechanism. The latter finding agrees with the earlier finding from the P-wave polarity pattern study.

However, an ongoing study of focal mechanisms of large events (M_L 0 to M_L 3, including rock bursts and nondamaging events) in the 99 stope at the Galena Mine shows that the standard, symmetric quadrupole model does not fit the observed data in all cases. For some large events, a quadrupole model is quite consistent with the data (figure 1*A*). Other large events appeared to yield a large distribution of dilatational arrivals on the focal sphere (figure 1*B*), which is more consistent with an implosional source mechanism. Still other large events appeared to yield a large distribution of compressional arrivals on the focal sphere (figure 1*C*) more consistent with an explosional source mechanism. Nearby (in time and space) microseismic events associated with a main event appeared to have the same type of focal sphere pattern as the main event in the few cases examined.

There are some possible explanations for the latter two sets of cases of deviation from a standard, symmetric quadrupole model. (1) The ray paths from the source region to at least some of the stations are highly contorted from the assumed straight path, (2) the source region deviates in a significant way from the assumed uniform isotropic model, and/or (3) the kinematics of the source is such that the assumption of slip on a planar surface is wrong. The first explanation is not favored because most microseismic events examined to date are largely consistent with the standard quadrupole model. If either (2) or (3) are correct, they may lead to a better understanding of certain kinds of large seismic events that result in rock bursts.

ENERGY RELEASE

Even though most of the seismic activity (in terms of number of events) in the mine occurs as microseismicity, most stored strain energy is released through infrequent rock bursts and other large events. For the smallest events detected (about M_L -5), the volume of rock that undergoes strain energy release is about 5×10^{-3} m^3 or a sphere about 0.2 m in diameter, which yields a few times 10^{-5} J of seismic energy. In contrast, for an M_L 3.0 event, the volume of strain energy release is about 2.5×10^7 to 4.5×10^7 m^3, or a sphere about 300 to 440 m in diameter (Swanson, 1992; Boler and Swanson, 1993a). Such a volume at the Galena Mine would encompass a number of

Figure 1
Equal-Area Focal-Sphere Plots of Selected Rock Bursts.

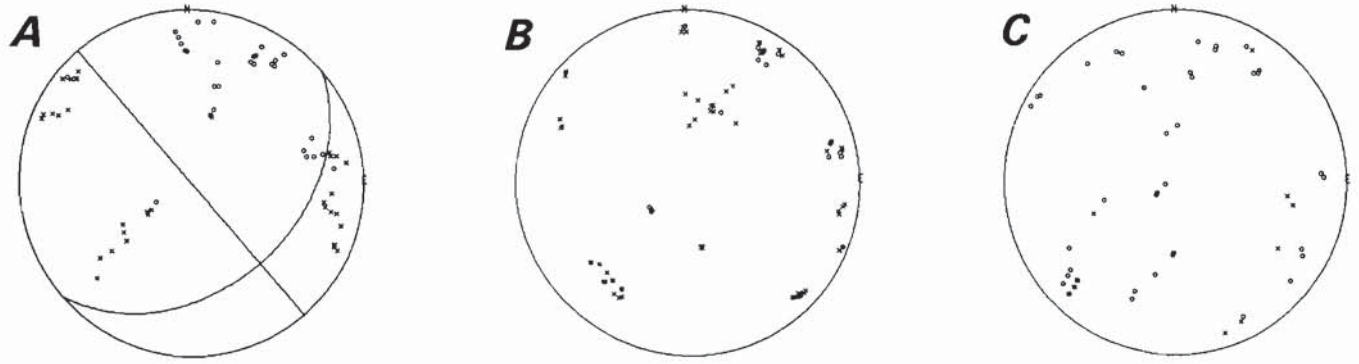

Composite upper hemisphere, equal-area focal-sphere plots of selected rock burst events in the 99 stope. Compressional arrivals at sensors are indicated by an "o," dilatational arrivals at sensors are indicated by an "x." *A*, M_L 0.9 event of February 7, 1990, as well as two foreshock and three aftershock microseismic events with P-wave quadrupole analysis; *B*, event of November 18, 1990, as well as one foreshock and two aftershock microseismic events with mainly dilatational arrivals; *C*, event of October 10, 1990, of two main events plus one aftershock with mainly compressional arrivals.

different working stopes on different levels. The energy release of the large events completely dominates the total; for a period of 18 months, 80 pct of the energy released along the main trend of the Galena Mine was released in just four events totaling over 2.8 GJ (Swanson, 1992). Using typical values of seismic efficiency of no greater than 0.1 down to 0.01, the total energy in these four rock bursts would have been roughly equivalent to the chemical energy in 10 to 100 t of TNT.

The occurrence of a large event significantly alters the state of stress in a volume of rock comparable to the volume involved in strain energy release. For example, at the Galena Mine, in the 10.5 h following one M_L 2.9 rock burst and using four stope arrays, over 4,000 microseismic events were detected and located by the routine monitoring system within about 200 m of the hypocenter of the main event (Swanson, 1992). The actual number of microseismic events within this volume of strain release was probably much larger because these four arrays only partially covered the volume.

MICROSEISMIC DECAY SEQUENCES

The decay of aftershocks following a large seismic event can be modeled as a modified-Omori decay:

$$n'(t) = k(t + c)^{-p},$$

where t is the elapsed time after the main event; $n'(t)$ is the number of aftershock events occurring per unit time; and k, c, and p are constants to be determined. An iterative approach using a maximum likelihood method can be used to determine the value of the constants (Ogata, 1983).

The idea of whether the microseismicity following a production blast or large seismic event in a mine follows a modified-Omori decay was tested by Satoh of the Geological Survey of Japan during a 3-month visit to DRC in 1991.[6] Satoh looked at data concerning events that were detected and located by the routine monitoring system around the 99 stope and collected over 11 months. Sixty-nine blasts and large events within this 11-month window were selected. Each had an uninterrupted sequence of microseismicity long enough to analyze. Satoh found that the microseismic decay following these events can, in fact, be fit by a modified-Omori decay model; figure 2 shows one of these fits following a routine production blast. Note that the routine monitoring system saturates at 12,000 events per hour because of the lower limit of 0.3 s/cycle of the SAIC unit, so that the calculated values of k and c have a much higher degree of uncertainty than is indicated by the fit.

[6]Satoh, T. Report of the Stay in Denver Research Center, U.S. Bureau of Mines, February to April 1991. USBM internal memorandum, 1991, 8 pp.

Figure 2

Example of Microseismicity Decay Following Production Blasting.

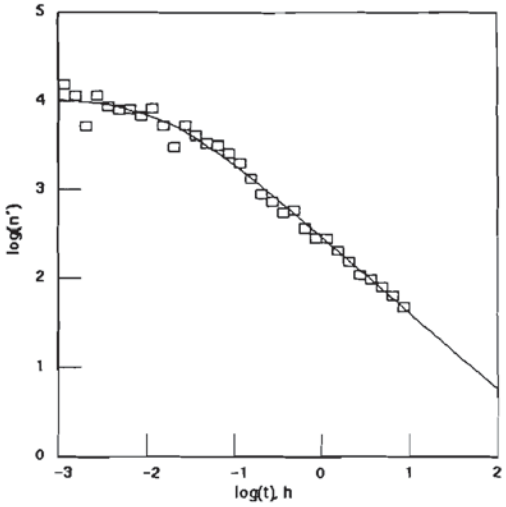

Modified-Omori decay fit (solid line) to typical post-production blasting microseismic event rate (n′ = events per hour) from data collected by routine monitoring system for the 99 stope. Data histogram is represented by rectangles. Saturation at 12,000 events per hour occurs owing to cycle time of the SAIC rock-burst monitoring unit. Three small rock bursts followed the blast, which was on April 30, 1990, at the end of day shift. The parameters of decay fit (with 1 σ uncertainty) are p = 0.860 (±0.021), k = 290.7 (±8.3), and c = 0.015 (±0.003).

It was found that the value of p (which indicates decay rate) of production blasts is indistinguishable from that of the larger seismic events at the mine (so-called bumps, including rock bursts). Satoh also noted that p for these decays (figure 3*A*) tended to yield a more tightly clustered distribution with a smaller mode (p of 0.8 to 0.9) than decays following large earthquakes (p of 1.3) (Utsu, 1969), meaning that microseismicity in this mining environment dies out more slowly than natural aftershocks.

Later analyses of these same microseismicity decays following production blasts indicate that a larger mode of p can be found if the modified-Omori fits are cut off at 2 or 1 h after the time of the blasts, yielding p modes of 0.9 and 1.0, respectively (figure 3*B* and *3C*, respectively). An anomalous rise in activity following many of the routine production blasts is observed to start about 1 to 8 h after the blasts. Two examples of this behavior are shown in figure 4.

The main motivation for this study was a recent finding that the foreshocks of the Loma Prieta earthquake had a smaller p than the aftershocks and that p changed from

Figure 3
Example of Time History of p Following Blasts and Bursts.

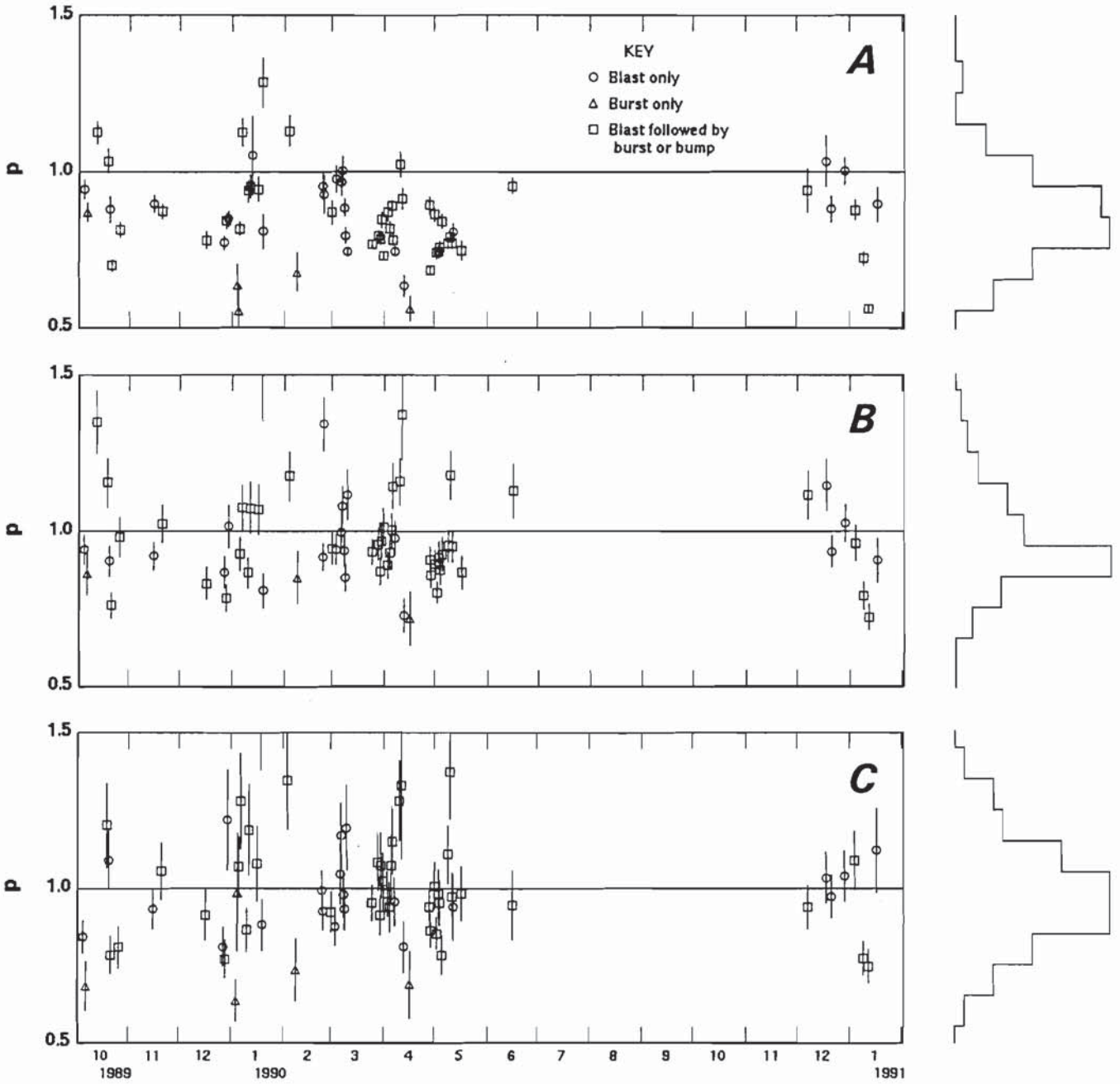

p of modified-Omori decays fit to blast and rock-burst sequences from October 1989 through January 1991 in the 99 stope. Vertical line at each p shows the 1 σ uncertainty. A relative histogram of the p-value distribution is shown at the left. *A*, Analysis of all data until next blast or burst, sometimes for sequences of 100 hours; *B*, termination of fit to events within 2 hours after main event; *C*, termination of fit to events within 1 hour after main event.

Figure 4
Example of Microseismic Decay Following Blasts With Increases in Rate.

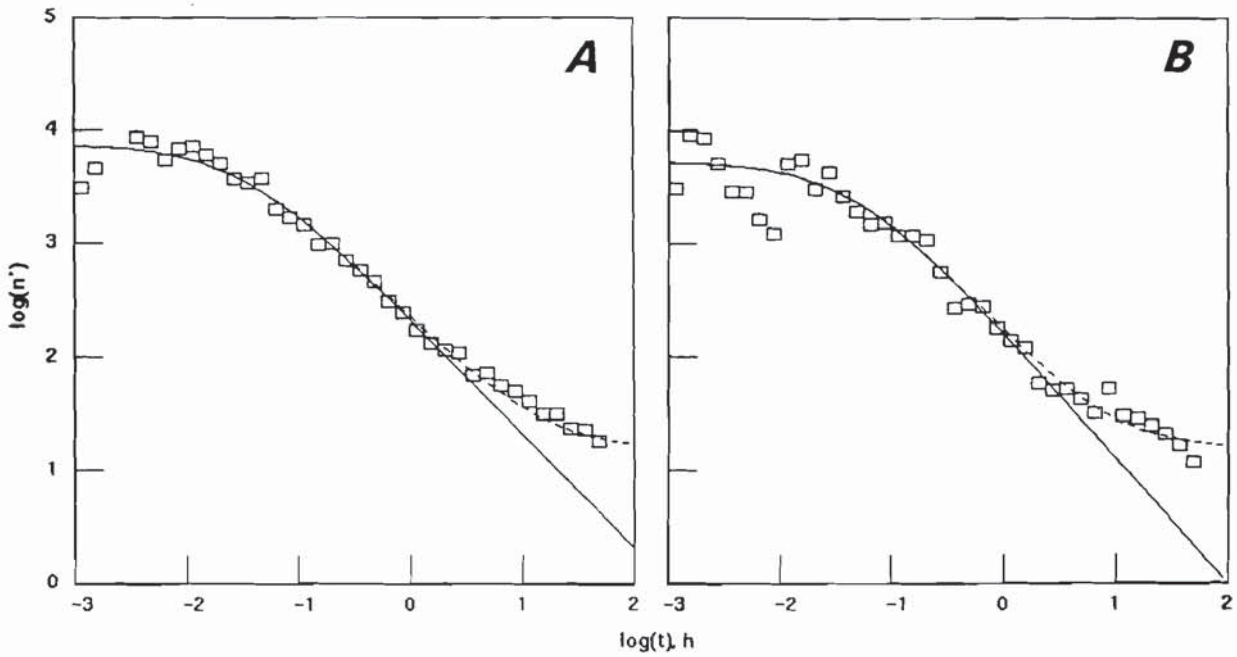

Same as figure 2, but for two other blasting events. Decay shows a break in slope at about 1-2 hours after the blasts. Dashed line is modified-Omori fit plus hypothetical constant rate of 15 events per hour. *A*, events following production blast on March 30, 1990, with a parameter fit of p = 1.011 (±0.060), k = 215.7 (±11.0), and c = 0.030 (±0.009); *B*, events following production blast on March 9, 1990, with a parameter fit of p = 1.116 (±0.080), k = 161.9 (±9.5), and c = 0.044 (±0.013).

about 0.6 to 1.1 at the time of the main event (Reasenberg, 1990). However, in the 99 stope area, there was no statistically significant temporal variation of p in the blast microseismic sequences before and after a burst.

TWO-DIMENSIONAL TOMOGRAPHY EXPERIMENT

Although the digital research system was designed for monitoring passively, the software was slightly modified to allow it to be used for one active source study (Billington and others, 1990b).[7] This study was designed to gauge the success of one or more planned destressing blasts in a vertical sill pillar above the 99 stope. This stope at the time of the planned destressing would be nearing the critical geometry for large rock bursts (outlined in "Introduction"), i.e., it would be about 25 to 30 m below the drift that would form one side of the horizontal pillar to be examined. The objective was to collect data both before and after the destress blast so that velocity tomograms of the horizontal pillar could be calculated. The difference tomogram would show where velocities changed: Increases in velocity might be due to increases of normal stress - thereby closing microcracks - and decreases in velocity might be due to an increase in microcrack population, showing internal damage to the pillar. An expected result was that if destressing the vertical sill pillar above the stope were successful, then an increase in stress somewhere in the horizontal pillar might be observed afterward.

To prepare sites for the tomographic sources and receivers, 30 jackleg holes were drilled from 0.6 to 1.2 m into the ribs of two drifts and one crosscut making up three sides of the horizontal pillar. The two drifts were the 104-vein drift in the vein under production (located above the planned destress blasts) and the 120-vein drift on the same level in a previously mined vein. The jackleg holes allowed the sources and receivers to be placed somewhat away from the highly fractured rind of rock that immediately surrounds mine openings in hard-rock mines. Magnetic stainless-steel plugs were affixed at the ends of the jackleg holes to provide the base for the active source (a tamping rod hit against the plug) and the receivers (Wilcoxon Research 793M-40 accelerometers) attached by magnets.

[7]Billington, S., F. M. Boler, P. L. Swanson, and L. H. Estey. A 2-D P-Wave Velocity Tomographic Experiment in a Deep Mine. Also presented at the Workshop on Induced Seismicity, 33rd U.S. Symp. Rock Mech., Santa Fe., NM, June 8-10, 1992.

To gain partial acoustic access to the fourth side of the pillar, two NX boreholes (7.49 cm in diameter) were drilled, one from the end of both drifts toward the end of the opposite drift. Into each borehole was placed one triaxial station made up of three mutually perpendicular 2 Hz to 25 kHz accelerometers.

The total pillar dimension that was scanned was about 60 by 90 m. The coordinates of all source and receiver sites were surveyed, and in most cases, the uncertainties of these coordinates were about ±0.05 m in all three directions. The majority of stations were clustered within ±0.3 m of a horizontal plane, though the total z-coordinate variation of the coordinates was about 2.7 m. The sampling frequency of the recorded waveforms was selected to be 50 kHz (equivalent to a spatial resolution in each waveform of about 0.1 m).

With the above array, 30 sites could be occupied as a source site, yielding 31 independent travel-time paths at each source site. For each tomographic image attempted, at least five separate impacts of the tamping rod were recorded at each source site. This amounts to about 5,000 waveforms per tomographic image. In all, data for three tomographic images were obtained, each data set being collected in less than two consecutive mining shifts on August 3, 1989, November 30, 1989, and February 13, 1990. The tomographic inversion was done with software developed by researchers at the USBM's Twin Cities Research Center (Jackson and others, 1992; Friedel and others, 1992), which allows for linear velocity gradients of an isotropic velocity within specified rectangular pixels on a plane.

These three tomographic data sets spanned four rock bursts in or near the 99 stope area, as well as two destressing blasts. The rock bursts occurred on October 5, 1989 (M_L 2.1), February 4, 1990 (M_L 1.2), and February 7, 1990 (M_L 2.9 followed 8.4 h later by an M_L 0.9 event). The destress blasts were done on December 15, 1989, and February 2, 1990, and caused immediate releases of seismic energy no greater than about M_L -0.5 and M_L 0.0, respectively. The first rock burst (M_L 2.1) had a source hypocenter near the corner of the pillar formed by the 120-vein drift and the crosscut and caused damage to the ribs in that area; the burst on February 4 (M_L 1.2) occurred off the end of the 104-vein drift; the first burst on February 7 (M_L 2.9) was about 60 m higher in the mine above one end of 120-vein drift; and the second burst on February 7th (M_L 0.9) was between the destress area of the vein and the 104-vein drift (Boler and Swanson, 1993a; 1993b).

The tomogram results can be summarized as follows. Each of the three tomograms have a low P-velocity region around most of both the drift and crosscut openings, a finding that is consistent with a fractured rind. The lowest P-velocities are near two raises in the 104 vein and at the corner formed by the 104-vein sill drift and the crosscut. There is also a high P-velocity core to the pillar. These results are very similar to those of a cruder P-velocity survey of a vertical sill pillar by Blake and others (1974) elsewhere in the mine. In the August 1989 tomogram, there is no indication of a high P-velocity area at or near the region where the future M_L 2.1 event was to occur in October. The main feature of the difference tomograms is a P-velocity decrease in the corner of the pillar damaged by the M_L 2.1 event, consistent with the damage on the ribs that had been observed immediately following the event.

Microseismic event activity, as determined by the routine monitoring system for the 99 stope in a ±3-m horizontal slice centered on the imaged pillar, was concentrated around the 104-vein drift. There was no concentration of microseismic activity in the area of the source of the M_L 2.1 event, neither before nor after the event occurred. Conversely, there was a concentration of microseismic activity in the area of the raise going down to the stope where the first difference tomogram (August 1989 to November 1989) shows a P-velocity increase. The second difference tomogram (November 1989 to February 1990), which brackets both destressing attempts in the sill pillar, shows only a slight increase in P-velocity in certain areas of the interior of the horizontal pillar. This increase also has no obvious correlation with microseismic activity at the time.

BPC MONITORING

The BPC array was fully operational during the time of the two rock bursts near the tomographic array on February 7, 1990. In addition, both microseismic systems were operational. Unfortunately, the first event (M_L 2.9) was not captured by the digital research system, as it was triggered 4 s earlier by a microseismic event near the 99 stope. This event was, however, captured by the routine monitoring system and was later located by using the arrival times recorded by that system and the location method used by the digital research system. A foreshock of the M_L 2.9 event, which was located in the same place as the main event, occurred about 40 min earlier and was captured by the digital research system. Using the P-wave polarity information from this foreshock of the M_L 2.9 event, and the M_L 0.9 event and its two foreshocks and three aftershocks, a focal mechanism was constructed for each large event. The strike of one of the nodal planes of each mechanism approximately matched the strike of the locally mapped, near-vertical faults in that part of the mine (Boler and others, 1990; Boler and Swanson, 1993a, 1993b).

For both the M_L 2.9 and M_L 0.9 events, a linear, three-dimensional dislocation model was used to compute expected coseismic pressure changes on each cell of the BPC array. The dislocation plane selected for each event

coincided with one focal mechanism nodal plane. The area of each dislocation plane was determined using an empirical magnitude-size relationship (Swanson, 1992). Then, a least squares fit was performed to find a scaling factor for the dislocation slip (and, for the M_L 2.9 event, to also find an orientation for the slip vector of the dislocation) that matched the coseismic pressure changes recorded on the BPC array. The final results show that the M_L 2.9 event can be modeled as 1.9 mm of combined left-lateral strike-slip and dip-slip over 88,000 m^2 of fault surface, and the M_L 0.9 event can be modeled as 0.5 mm of combined left-lateral strike-slip and dip-slip over 780 m^2 of fault surface (Boler and Swanson, 1993b).

Another important result of these dislocation models is that the M_L 2.9 event may have enhanced the likelihood that the later M_L 0.9 event would occur. This might have been caused by the dislocation motion of first event, which modified the stress across the future fault surface of the future M_L 0.9 event, lowering by 0.1 to 0.2 MPa the normal stress and also increasing by 0.4 MPa the particular shear stress component that led to the observed sense of dip-slip fault motion. However, the dislocation model of the M_L 2.9 event also yields a decrease of 0.3 MPa in the shear stress leading to left-lateral strike-slip motion on the plane of the M_L 0.9 event, which would have inhibited the fault-plane motion observed in the M_L 0.9 event.

STOPE CLOSURE MONITORING

A strong time correlation was found between stope closure as monitored with the convergence gages and the largest events occurring around the 99 stope (Boler and Swanson, 1992). In particular, the largest coseismic closure was 1.25 mm associated with an M_L -1 event located less than 10 m away from one of the gages. Closures of 0.2 mm were observed for an M_L 2 event located in another stope 190 m away. Coseismic convergence was observed for events down to about M_L -2. Also noted was that the convergence rates of the gages correlate with the position of the production face. However, aseismic creep (i.e., creep with no detected or associated seismicity) accounted for 18 pct of the total closure of one gage and 65 to 70 pct of the closure of the other two gages.

LARGE DOUBLET EVENTS

A doublet is defined here as two large events of significant magnitude and rock-burst potential occurring in about the same place in the mine and separated in time by a few minutes to a few days. Large doublet events (and in some cases, multiplet events) occurred in many areas in the Galena Mine. Figure 5 shows the occurrence of large doublets over a 20-month period in a stope that was not being monitored for microseismicity. About half the large

Figure 5
Example of Doublet Sequence for One Stope.

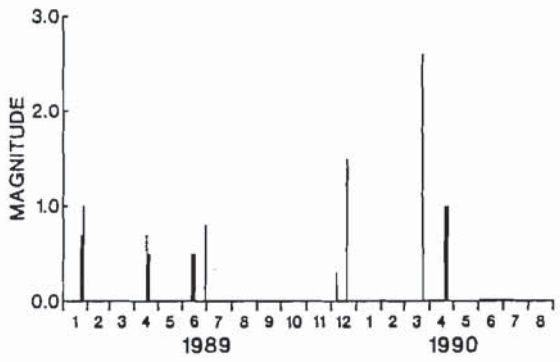

Sequence of rock bursts for the 49-133 stope area for a 20-month period. Local magnitudes were determined from surface seismograph records. Four sets of closely spaced bursts are identified as "doublets" (see text). Time interval between the two events of each doublet is actually less than 24 h.

events of M_L greater than 1 throughout the mine over this same time period were doublets that occurred within 24 h of one another (Swanson and Sines, 1990, 1991).

Two models were considered for explaining these large doublet events. One model relies on the modification of the local stress field on an existing fault surface resulting from the motion of the first event (Swanson, 1992; Boler and Swanson, 1993a, 1993b), as discussed above for the M_L 2.9 and M_L 0.9 events in the 99 stope. The other model relies on two facts: (1) Many of the veins in the Galena Mine are roughly perpendicular to bedding plane faults, and (2) many of stopes in these veins are roughly normal to direction of the large horizontal principal stress in the mine. In this model, the compliance of the stope results in a stress concentration around the end of the stope that favors dislocation slip on a plane approximately perpendicular to the main trend of the stope. Thus, at the Galena Mine, when a stope face would advance to the vicinity of a critically stressed bedding fault, the fault on one side of the stope may have been activated, followed shortly by activation of the fault on the other side. The probability of activation of the second half of the fault increases in both models discussed here. Given the ubiquitous presence of faults in the Galena Mine, it is difficult to determine which of these two models is correct (if either).

EVIDENCE OF STATE OF CRITICALITY

This section describes several examples showing that the rock surrounding recently mined openings has faults and fractures in a state of criticality, so that minor perturbations in stress or strain appear to induce seismic activity on some of these faults and fractures. Taken

together, these examples suggest that minor or distant (and seemingly insignificant) changes or activities in the mine environment can have a profound impact on inducing local seismic activity—even though the induced stress from these changes or activities is very small. It is important to realize that we are conjecturing real increases in seismic activity apparently resulting from increases in cultural activity in the mine (including both mining activity such as barring down, drilling, rock bolting, etc., and other activity such as movement of motors and ore cars, opening and closing of air doors, etc.), i.e., the increases in seismic activity are not a result of mistaking the noise of cultural activity for real seismic activity associated with rock fracture or slip.

(1) Prior to the resumption of mining in the 99 stope after a hiatus of over 2-1/2 years, a miner was sent into the stope to bar down loose rock. The miner reported a sharp increase in rock noise—or acoustic microseismicity—in the stope as the barring down took place. The stope had been quiet prior to this time.

(2) An increase in microseismicity in one stope has been observed to coincide with a production blast in another, nearby stope. For example, four adjacent stopes being simultaneously monitored by the routine monitoring system were selected for study. We noted that even when there had been no production blast in a certain stope, a flurry of microseismic activity in that stope would often occur at the time of production blasting (at the end of shift) when there was blasting in one or more of the other three stopes. The located events are deemed not to be a numerical artifact of a stope system mislocating events around another stope, as the detection times for these events do not correlate with the detection time for events in any of the other stopes.

(3) A statistical observation of the effect noted in (2) can be achieved by using a modified-Omori decay model. As discussed in the section on "Microseismic Decay Sequences," decay cutoffs of 1 to 2 h were used to fit microseismicity after routine production blasts. This was because, in many cases, a kink in the decay curve can be seen in which the data deviate from a modified-Omori decay fit about 1 to 8 h after the blast in the stope (figure 4). This 1- to 8-h period brackets the onset of increased cultural activity throughout the mine at the beginning of the next shift (1 h) and the time of blasting at the end of the next shift (8 h). Although a constant background of 15 to 20 events per hour could account for this kink in the modified-Omori curves (figure 4), a constant background is not deemed to be a reasonable explanation owing to the occasional lack of this kink following some blasts (e.g., figure 2). In fact, as seen in figure 4*B*, the data after the point of the kink resemble a small, new, modified-Omori curve, suggesting activation of a small, new source region.

(4) The occurrence of sympathetic activity suggested by (2) and (3) above may not be limited to small microseismic events. At the other end of the spectrum, as discussed in the section "BPC Monitoring" (M_L 0.9 event in the 99 stope following a nearby M_L 2.9 event) and in Swanson and Sines (1990) and Swanson (1992), there is evidence to support an increase in the probability of occurrence of large events from the occurrence of other nearby large events. The data compiled by Swanson (1992) show that between January 1989 and May 1992, there were several other occurrences of bursts within a short window of time in the same or different stopes of the mine where the subsequent event occurred at a time of enhanced cultural activity in the mine (but not at blast time). The question then arises: Why does the second event in the doublet occur when it does? Do minor stress perturbations due to the cultural activity sometimes trigger the subsequent event, or is the occurrence of this event at these times of cultural activity just a random happening? We do not yet have an answer to these questions.

FRACTALITY, CLUSTERING, AND PLANARITY OF MICROSEISMIC EVENTS

To better understand the response of the damaged rock mass in the neighborhood of active stopes, microseismicity was examined using various statistical methods to characterize spatial and temporal activity after blasts and rock bursts in the vicinity of these stopes (Coughlin and Kranz, 1991; Kranz and others, 1994). These methods attempt to characterize a sequence of events following a progenitor (blast or burst) as a whole and do not rely on details of individual microseismic events. The data archived by the routine monitoring system are ideal for these methods because waveform analysis is not required.

One finding using these methods is that microseismic activity around stopes has a fractal or self-similar nature in time and space. In time, the fractality extends over scales at least from minutes to days, where these temporal scales are currently limited by the inability to capture and detect all seismic activity immediately after a blast or burst at the smallest scale and the interference of effects from subsequent blasts or bursts at the largest scale. In space, fractality extends over scales from 1 to 100 m, where these spatial scales are currently limited by event location precision at the smallest scale and the array size at the largest scale. There appears to be no statistical difference in the distributions of fractal dimensions in comparisons of microseismic sequences following blasts and seismic events (including those involved in rock bursts) and no differences in the distributions of fractal dimensions in

comparisons of data from different stope arrays. This result suggests that the physical processes responsible for rock mass relaxation following a sudden stress change in the mine are the same, regardless of the stress change progenitor or the stope location.

An ongoing study, however, is revealing that different attributes of this relaxation response may vary depending on whether the progenitor is a rock burst or a blast and may also vary from stope to stope. Differences in attributes that measure spatial extent, event decay rate, accumulative event counts, and the energy of these sequences are found. On the other hand, the attributes of fractal dimension are indistinguishable. This suggests that there are methods to characterize the rock mass in a mining environment by characterizing microseismicity and that any such characterization will be independent of the progenitor of the microseismicity.

Billington and others (1990a) showed that it was possible to identify and map active faults within the country rock (within the coverage of an array) by identifying concentrations of microseismic events outside of normal stope activity. The locations of these active faults can be found to the same degree of accuracy as the locations of microseismic events, i.e., a few meters. The more rigorous methods of Kranz and others (1994)[8] show that microseismicity in different stopes usually has a primary planarity that approximates that of the vein being mined, which agrees with the work of Billington and others (1990a), and that the microseismic planarity is the same regardless of the progenitor. Routine identification of bedding plane faults by this method is rare. Several interpretations of why the bulk of the microseismicity in a stope approximates the vein are currently being investigated.

BEHAVIOR SINCE JULY 1992

The initiation of standby mode at the Galena Mine in mid-1992 afforded an opportunity to continue monitoring microseismicity at the mine in the absence of development and production blasting. Microseismicity continued even in the absence of large events. Also, microseismicity decays continued to follow a modified-Omori decay law, lending support to the premise that the kinks at 1 to 8 h in the decays of stope activity during production were in fact due to activation of microseismic slip from blasting and cultural activities elsewhere in the mine and were not due to background activity.

Data from the 99 stope array are used to illustrate these points. The 99 stope array is selected because there were no changes in station number or station position during the period of time shown (figures 6 and 7), and there were relatively few large data gaps resulting from power outages and other hardware problems. The few main data gaps are in mid-September 1992 (100.3-h gap), mid-November 1992 (49.5-h gap), early May 1993 (75.1-h gap), mid-May 1993 (160.2-h gap), and late June 1993 (31.6-h gap).

Microseismic activity decays smoothly in the 99 stope following the last blast in the afternoon of June 3, 1992. A near-constant rate of activity occurs for about the next 100 h or so, probably corresponding to sympathetic activity induced by blasting in nearby areas. This activity finally ceases by mid-June 1992, and the activity steadily decays following a power-law decrease ($p \sim 0.76$) until the occurrence of an M_L 3.0 rock burst in the afternoon of March 18, 1993.

The decay of microseismic activity following the March 18 event is shown in figure 8. The decay is a near-perfect power law also with a p of about 0.76, because the two low points of the decay are due to the data gaps in May and June 1993.

A second M_L 3.0 rock burst occurred about 280 m from the 99 stope on July 1, 1993, a year after the cessation of routine blasting at the mine. The decay of microseismic activity following this event is shown in figure 9. Here there seems to be two different rates of decay. The first has a p about equal to that following the March 18 event, ending about 30 h after the main event; the second has a p of about 0.45.

Three other small rock bursts (M_L 0.0 $\pm$0.5) occurred elsewhere in the mine on September 6, 1992, September 10, 1992, and January 20, 1994. These events did not affect the event rate in the 99 stope.

These results, combined with the earlier microseismic decays during production, suggest that the mine has two or possibly three different inherent damage structures. The interpretation of the various values of p (1.0, 0.76, and possibly 0.45) is still being investigated.

PRECURSOR ACTIVITY BEFORE ROCK BURSTS AND OTHER LARGE EVENTS

The main underlying assumption that led to the intense microseismic monitoring effort at the Galena Mine was the belief that some type of microseismic precursor activity would occur and would be detectable prior to large seismic events, allowing for an acceptable amount of time to relocate mine personnel to avoid or reduce the possibility of injury. For example, models of source preparation and laboratory experiments indicate that there should be an acceleration of small events prior to a main event. In fact, at the Galena Mine on at least one occasion, an increase in activity did occur. On January 3, 1990, a sharp increase in microseismic activity occurred 2 to 3 h prior to the first of two small rock bursts (M_L -0.5 or less) at the face of

[8]See also footnote 5.

Figure 6
Microseismic Event Decay During Standby at Galena Mine in One Stope.

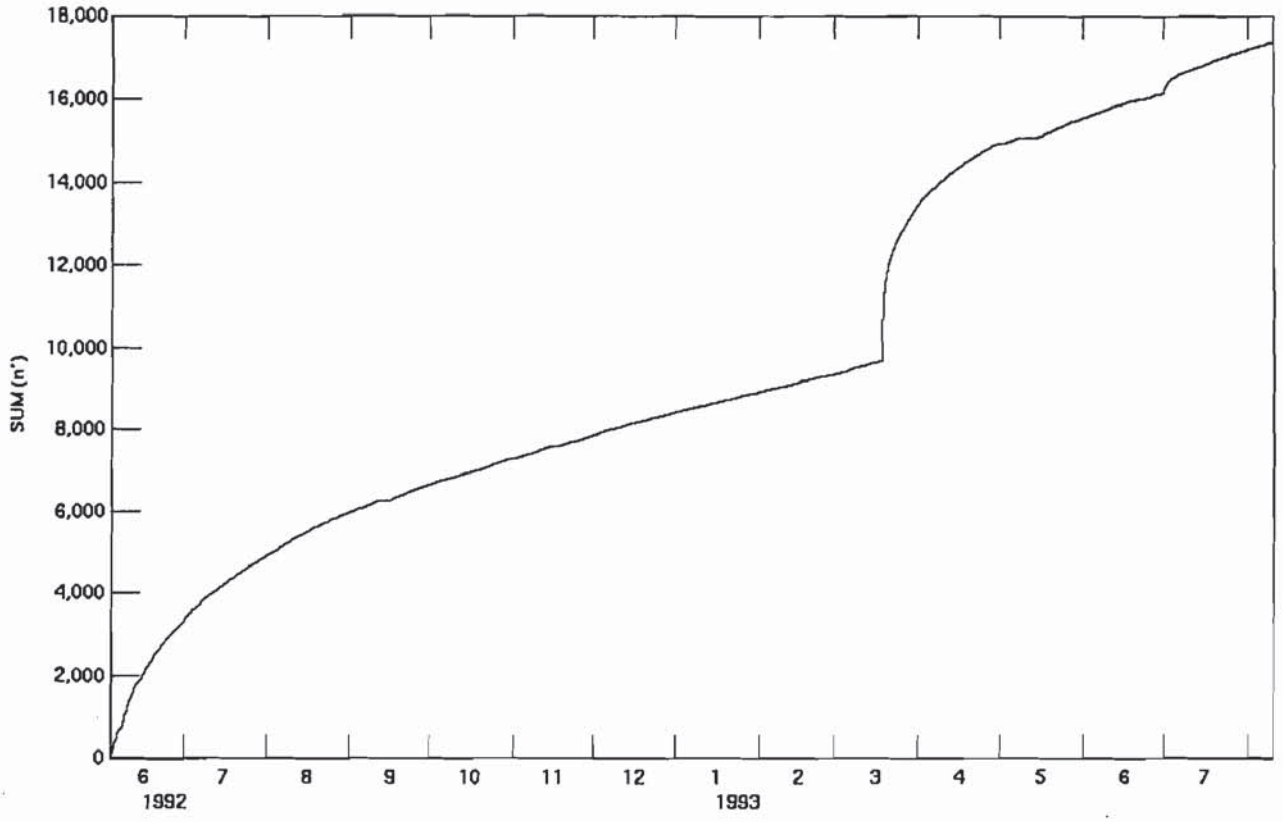

Accumulative number of located microseismic events in 99 stope area following the last blast in the stope, following day shift on June 3, 1992. A few periods of zero accumulation are due to data gaps (see text). The increases in March and July 1993, coincide with a M_L 3.0 event on March 18 in stope area and another M_L 3.0 event about 280 m away on July 1.

the 99 stope. This stope was being monitored by the routine monitoring system at the time. The increase in activity alerted personnel in the instrumentation room, so there was time to contact the miners in this stope and suggest they take an early lunch. Thus, no one was working at the face at the time when the first burst occurred, and work in the stope was suspended for the rest of the day. However, the microseismic activity of the stope had dropped almost to the normal background rate by the time of the first burst, i.e., there was no continuing buildup in activity leading up to the main event.

An attempt was made to identify in a consistent fashion any change, whether an increase or a decrease, in microseismic activity that may have occurred prior to 35 large seismic events in the mine having an M_L from about 1 to 3 (Swanson, 1993). This study included the two M_L 3.0 events that occurred after the Galena Mine went into standby mode, but excluded the two small events of January 3, 1990. Microseismic activity was found to increase in the days and weeks prior to some of these large events, probably because of increases in local stress concentrations as a result of mining. However, no obvious increase in activity was found to occur in the seconds to 2 h preceding these large events. In fact, microseismic activity before these events was completely consistent with the activity expected from a modified-Omori decay following the last mining blast or large event in the area. If the accumulative number of microseismic events occurring during the 2 h before these 35 large events are stacked, a near-linear increase in accumulative microseismic events is found, which indicates a near-zero rate of change in average activity prior to these events. Thus, contrary to predictions of failure models, results of laboratory experiments, and our predilections, there is not a consistent acceleration of small events before large events at the Galena Mine. If there is accelerating creep-like deformation in the moments before a large main event in the mine, this acceleration is accompanied by microseismic events that are no larger than 7 to 9 orders of magnitude smaller in energy than the main event.

Figure 7
Microseismic Event Decay From June 3, 1992 Through March 18, 1993.

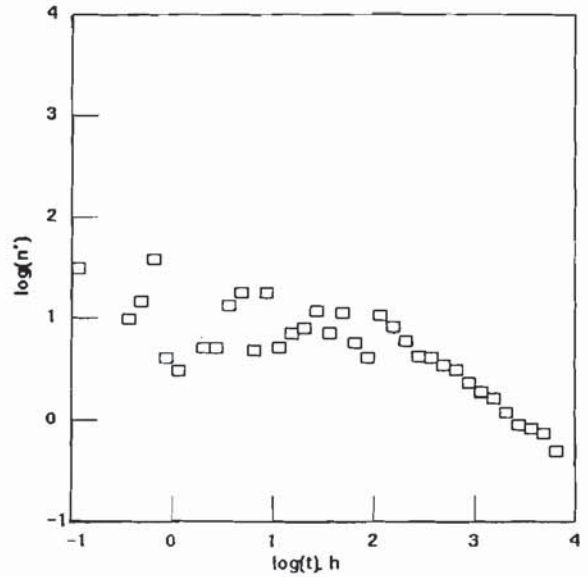

Histogram of microseismic decay rate for located events in 99 stope area following the last blast. The decay starting at about 100 h after the last blast probably signifies end of sympathetic activity resulting from blasting in nearby areas and has a p of about 0.76.

CONSIDERATION OF LARGE ASEISMIC DEFORMATIONS

The studies of Swanson (1992) and Boler and Swanson (1993a, 1993b) show the significant changes in slip potential that can result in different areas of the mine as compliant mine openings deform and dislocation motion takes place in other parts of the mine. It is vital to note that although these studies are attempts to model the changes in slip potential resulting from large seismic events in the mine, there is nothing to limit the overall conclusions as resulting from only seismic events. In fact, at the Galena Mine, a large amount of aseismic deformation (up to several centimeters per year) would routinely take place in certain areas. These areas tended to be in the soft St. Regis Formation and thus tended not be rock-burst prone and transmitted only a small amount of rock noise. Therefore, none of these areas were instrumented to monitor microseismicity. But to understand the driving mechanisms that affect rock-burst-prone areas, these aseismic areas are just as relevant as seismic areas and require an understanding of the overall deformation of the mine. In short, monitoring and understanding the seismic component of deformation represents only part of the overall problem of monitoring and understanding rock bursts.

Figure 8
Microseismic Event Decay From March 18 Through July 1, 1993.

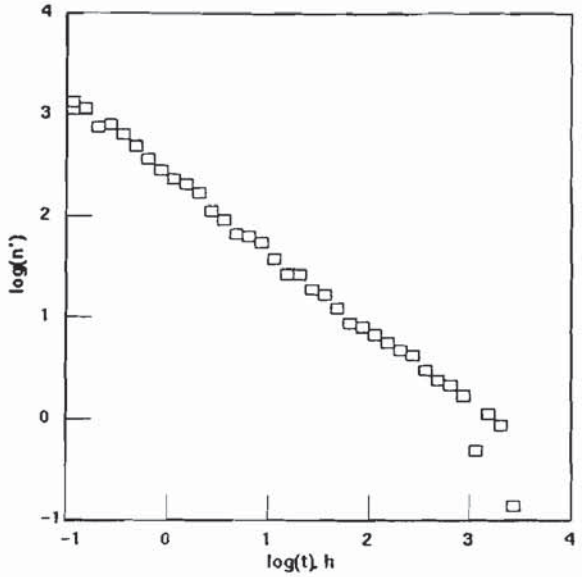

Histogram of microseismic decay rate for located events in 99 stope area following the March 18, 1993, M_L 3.0 rock burst. This decay also has a p of about 0.76.

Figure 9
Microseismic Event Decay Following July 1, 1993.

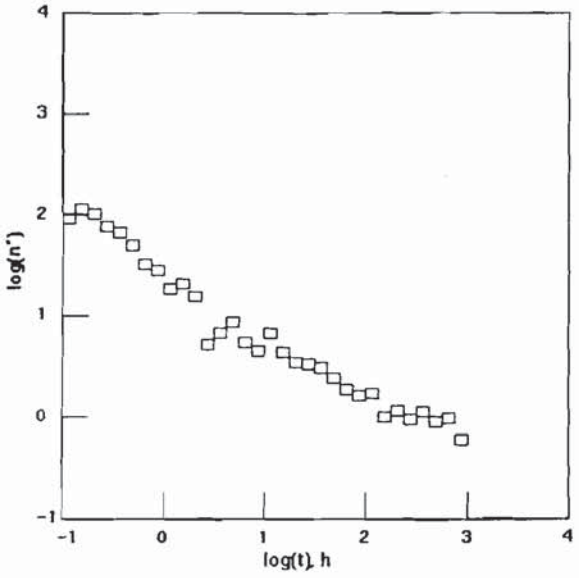

Histogram of microseismic decay rate for located events in 99 stope area following the July 1, 1993, M_L 3.0 rock burst 280 m distant. This decay appears to have two power-law segments; first has a p of about 0.76; second starting about 30 h after the main event, has a p of about 0.45.

SUMMARY AND FUTURE DIRECTIONS

Two types of microseismic monitoring systems were designed, tested, and used to monitor a number of rock-burst-prone stopes at the Galena Mine. Much of the data collected with these systems has been archived and continues to be a valuable resource for study to elucidate aspects of the rock-burst problem. One of the systems uses an array of receivers to detect and locate events automatically and then archives the data, as well as some statistical information about each event. The other system collects digital waveform data from the array, which allows for a more complete analysis of each event, and can be used to collect and analyze other dynamic and quasistatic measurements at the same time microseismic activity is being monitored. The data collected by each system are complementary and are amenable to a suite of different analysis methods.

The idea that there might be some type of anomalous microseismic activity before a rock burst has been tested in a variety of ways. Whereas isolated cases have been identified in which there was a sudden increase in activity before a burst, there appears to be no unique, reliable, easily detectable, or statistically significant occurrence of anomalous microseismic activity before rock bursts at the Galena Mine. Thus, a reliable short-time indicator of an impending rock burst that would allow for the safe relocation of personnel in the area does not yet exist.

However, several methods of analysis suggest that there are ways to forecast changes in the likelihood of the occurrence of rock bursts. One such method is the characterization of the rock mass around a stope through the use of microseismic events; moreover, this characterization seems to be statistically independent of the progenitor of the microseismic events. Nearly all microseismic events and many rock bursts appear to occur by slip on a plane, whether on preexisting faults or bedding planes, or on surfaces resulting from new fracture. Changes in slip potential on preexisting fault or bedding surfaces resulting from either seismic or aseismic deformation in other regions of the mine can be calculated. The seismic component is readily amenable to study by analysis methods already developed for full waveform data, but the aseismic component will be very difficult to measure and characterize for an entire mine. Our understanding of the problem at this time leads us to think that a simultaneous monitoring of both the seismic and the aseismic deformations in a mine such as the Galena (where significant amounts of both types of deformation occur) will be required in order to estimate accurately any changes in slip potential in the rock-burst-prone areas of the mine and then to correlate these predicted changes with the actual occurrence of large seismic events. Also, the source mechanisms of some rock bursts and associated microseismic events are not understood at this time; an active part of ongoing research is focused toward gaining an understanding of these different types of mechanisms. The problem remains to fully identify, characterize, and measure the mechanics of the geologic and mining-induced structures using both seismic and aseismic components of mine deformation.

REFERENCES

Aki, K., and P. G. Richards. Quantitative Seismology: Theory and Methods. V. 1, W. H. Freeman, 1980, 557 pp.

Billington, S., F. M. Boler, P. L. Swanson, and L. H. Estey. P-Wave Polarity Patterns from Mining-Induced Microseismicity in a Hard-Rock Mine. Paper in Rock Mechanics Contributions and Challenges: Proceedings of the 31st U.S. Symposium, ed. by W. A. Hustrulid and G. A. Johnson (CO Sch. Mines, Golden, CO, June 18-20, 1990). Balkema, 1990a, pp. 931-938.

____. 2-D P-Wave Velocity Tomographic Experiment in an Idaho Silver Mine. Abstract in Trans. Am. Geophys. Union, EOS, v. 71, 1990b, p. 1454.

Blake, W. Rock Burst Research at the Galena Mine, Wallace, Idaho. USBM TPR 39, 1971, 22 pp.

Blake, W., F. Leighton, and W. I. Duvall. Microseismic Techniques for Monitoring the Behavior of Rock Structures. USBM Bull. 665, 1974, 65 pp.

Boler, F. M., and P. L. Swanson. A CAMAC-Based Workstation for Microseismic and Acoustic Emission Research. USBM IC 9262, 1990, 9 pp.

____. Observations of Heterogeneous Stope Convergence Behavior and Implications for Induced Seismicity. Pure and Appl. Geophys., v. 139, No. 3/4, 1992, pp. 639-656.

Boler, F. M., and P. L. Swanson. Seismicity and Stress Changes Subsequent to Destress Blasting at the Galena Mine and Implications for Stress Control Strategies. USBM RI 9448, 1993a, 21 pp.

____. Modeling of a Destress Blast and Subsequent Seismicity and Stress Changes. Paper in Rockbursts and Seismicity in Mines 93. Proceedings of the 3rd International Symposium on Rockbursts and Seismicity in Mines, ed. by R. P. Young (Kingston, ON, Aug. 16-18, 1993). Balkema, 1993b, pp. 35-40.

Boler, F. M., P. L. Swanson, and S. Billington. Patterns of Microseismicity in an Idaho Silver Mine. Abstract in Trans. Am. Geophys. Union, EOS, v. 69, 1988, p. 1050.

Boler, F. M., P. L. Swanson, S. Billington, and L. H. Estey. Seismicity and Stress Changes Associated With an ML 2.9 Rock Burst in an Idaho Silver Mine. Abstract in Trans. Am. Geophys. Union, EOS, v. 71, 1990, pp. 1453-1454.

Coughlin, J., and R. Kranz. New Approaches to Studying Rock Burst-Associated Seismicity in Mines. Paper in Rock Mechanics as a Multidisciplinary Science: Proceedings of the 32nd U.S. Symposium, ed. by J. C. Roegiers, (Univ. OK, Norman, July 10-12, 1991). Balkema, 1991, pp. 491-500.

Coughlin, J., and C. D. Sines. Field Trials of a Portable Microseismic Processor Recorder. USBM IC 9022, 1985, 8 pp.

Engdahl, E. R., and W. A. Rinehard. Seismicity Map of North America Project. Ch. 2., Neotectonics of North America. Geol. Soc. Am., 1991, pp. 21-28.

Estey, L. H. Seismic Source Locations: The Fallacy of the Assumption of Minimum Travel-Time Residuals. Abstract in Trans. Am. Geophys. Union, EOS, v. 71, 1990, pp. 1479-1480.

Estey, L. H., P. L. Swanson, F. M. Boler, and S. Billington. Microseismic Source Locations: A Test of Faith. Paper in Rock Mechanics Contributions and Challenges: Proceedings of the 31st U.S. Symposium, ed. by W. A. Hustrulid and G. A. Johnson (CO Sch. Mines, Golden, CO, June 18-20, 1990). Balkema, 1990, pp. 939-946.

Friedel, M. J., D. R. Tweeton, M. J. Jackson, J. A. Jessop, and S. Billington. Mining Applications of Seismic Tomography. (Pres. at Ann. Meet., Soc. Explor. Geophys., New Orleans, LA, 1992). Extended Abstr., Soc. Explor. Geophys., 1992, pp. 58-62.

Godson, R. A., M. C. Bridges, and B. M. McKavanagh. A 32-Channel Rock Noise Location System. Paper in Proceedings, Second Conference on Acoustic Emission/Microseismic Activity in Geologic Structures and Materials, ed. H. R. Hardy, Jr., and F. W. Leighton (PA State Univ., University Park, PA, Nov. 13-15, 1978). Ser. on Rock and Soil Mech., v. 5., Trans Tech Pub., 1980, pp. 117-161.

Haramy, K. Y., and R. O. Kneisley. Hydraulic Borehole Pressure Cells: Equipment, Technique, and Theories. USBM IC 9294, 1991, 26 pp.

Hobbs, S. W., A. B. Griggs, R. E. Wallace, and A. B. Campbell. Geology of the Coeur d'Alene District, Shoshone County, Idaho. U. S. Geol. Surv. Prof. Paper 478, 1965, 139 pp.

Jackson, M. J., D. R. Tweeton, and S. Billington. Seismic Crosshole Tomography using Wavefront Migration and Fuzzy Constraints: Application to Fracture Detection and Characterization. Paper in Proceedings of the 6th National Outdoor Action Conference on Aquifer Restoration, Ground Water Monitoring, and Geophysical Methods. Nat. Groundwater Assoc., 1992, pp. 741-754.

Kranz, R. L., J. Coughlin, and S. Billington. Studies of Stope-Scale Seismicity in a Hard Rock Mine, Part I: Methods and Factors. USBM RI 9525, 1994, 27 pp.

Lee, W. H. K. (ed.) IASPEI Software Library Volume 1: Toolbox for Seismic Data Acquisition, Processing, and Analysis. Int. Assoc. Seismo. Phys. Earth's Interior, 1989, 283 pp.

Lee, W. H. K., D. M. Tottingham, and J. O. Ellis. A PC-Based Seismic Data Acquisition and Processing System. U.S. Geol. Surv. OFR 88-751, 1988, 31 pp.

Leighton, F. W. A Case History of a Major Rock Burst. USBM RI 8701, 1982, 14 pp.

____. Rock Burst Research at the Galena Mine–1976. USBM TPR 10020, 1976, 29 pp.

Lourence, P. B., S. J. Jung, and K. F. Sprenke. Source Mechanisms at the Lucky Friday Mine: Initial Results from the North Idaho Seismic Network. Paper in Rockbursts and Seismicity in Mines 93. Proceedings of the 3rd International Symposium on Rockbursts and Seismicity in Mines, ed. by R. P. Young (Kingston, ON, Aug. 16-18, 1993). Balkema, 1993, pp. 217-222.

Ogata, Y. Estimation of the Parameters in the Modified Omori's Formula for Aftershock Frequencies by the Maximum Likelihood Procedure. J. Phys. Earth, v. 31, 1983, pp. 115-124.

Reasenberg, P. A., Microclusters and Compound Clusters. Abstract in Trans. Am. Geophys. Union, EOS, v. 71, 1990, p. 1457.

Riefenberg, J. A Simplex Method-based Algorithm for Source Location of Microseismic Events Associated with Underground Mining. Paper in Rock Mechanics as a Guide for Efficient Utilization of Natural Resources: Proceedings of the 30th U.S. Symposium, ed. by A. W. Khair (WV Univ., Morgantown, WV, June 19-22, 1989). Balkema, 1989a, pp. 655-662.

____. A Simplex-Method-Based Algorithm for Determining the Source Location of Microseismic Events. USBM RI 9393, 1989b, 12 pp.

Rowell, G. A., and L. P. Yoder. The Effect of Geophone Emplacement on the Observed Frequency Content of Microseismic Signals. Paper in Acoustic Emission/Microseismic Activity in Geologic Structures and Materials: Proceedings of the Third Conference, ed. by H. R. Hardy, Jr., and F. W. Leighton (PA State Univ., University Park, PA, Oct. 5-7, 1981). Ser. on Rock and Soil Mech., v. 8, Trans Tech Publ., 1984, pp. 707-727.

Steblay, B. J, B. T. Brady, and E. E. Hollop. A Networked Minewide Microseismic Rock Burst Monitoring System. Paper in Mining for the Future: Trends and Expectations. (Proc. 14th World Min. Congr., Beijing, China, May 14-18, 1990). Pergamon, 1990a, pp. 861-868.

Steblay, B. J, B. T. Brady, and T. J. Swendseid. Innovative Microseismic Rockburst Monitoring System. Paper in Rockbursts and Seismicity in Mines, Proceedings of the 2nd International Symposium on Rockbursts and Seismicity in Mines, ed. by C. Fairhurst (Univ. MN, Minneapolis, MN, June 9-10, 1988). Balkema, 1990b, pp. 259-262.

Stickney, M. C. Montana Seismicity 1989. MT Bur. Mines and Geol. OFR-263, 1993, 46 pp.

Swanson, P. L. Mining-Induced Seismicity in Faulted Geologic Structures: An Analysis of Seismicity-Induced Slip Potential. Pure and Appl. Geophys., v. 139, No. 3/4, 1992, pp. 657-676.

____. Search for Accelerating Deformation in the Seconds Prior to Mining-Induced Seismic Events. Abstract in Trans. Am. Geophys. Union, EOS, v. 74, 1993, p. 411.

Swanson, P. L., and F. M. Boler. Application of AE/MS Waveform Analysis to Hazard Detection, Evaluation, and Control in Underground Mines. Paper in Process in Acoustic Emission IV (Proc. 9th Int. Acous. Emiss. Symp., Kobe, Japan, Nov. 14-17, 1988). 1988a, pp. 303-310.

____. Opportunities for Observation of Fault Activation in an Underground Mine. Abstract in Trans. Am. Geophys. Union, EOS, v. 69, 1988b, p. 1050.

Swanson, P. L., L. H. Estey, F. M. Boler, and S. Billington. Accuracy and Precision of Microseismic Event Locations in Rock Burst Research Studies. USBM RI 9393, 1992a, 40 pp.

____. Mining-Induced Microseismic Event Location Errors: Accuracy and Precision of Two Location Systems. Pure and Appl. Geophys., v. 139, No. 3/4, 1992b, pp. 375-404.

Swanson, P. L., and C. D. Sines. Repetitive Seismicity (M – 2-3) and Rock Bursting along a Plane Parallel to Known Faulting in the Coeur d'Alene District, ID. Abstract in Trans. Am. Geophys. Union, EOS, v. 71, 1990, p. 1453.

____. Characteristics of Mining-Induced Seismicity and Rock Bursting in a Deep Hard-Rock Mine. USBM RI 9393, 1991, 12 pp.

Utsu, T. Aftershocks and Earthquake Statistics, Part I: Some Parameters which Characterize an Aftershock Sequence and Their Interpretations. J. Fac. Sci. Hokkaido Univ., v. 3, 1969, pp. 129-195.

Special Publication 01-95

Proceedings: Mechanics and Mitigation of Violent Failure in Coal and Hard-Rock Mines

Edited by Hamid Maleki, Priscilla F. Wopat, Richard C. Repsher, and Robert J. Tuchman

UNITED STATES DEPARTMENT OF THE INTERIOR
Bruce Babbitt, Secretary

BUREAU OF MINES
Rhea L. Graham, Director

Library of Congress Cataloging in Publication Data:

Maleki, Hamid N.

Proceedings : mechanics and mitigation of violet failure in coal and hard-rock mines / edited by Hamid Maleki ... [et al.].

p. cm. — (USBM special publication; 01-95)

Includes bibliographical references.

Supt. of Docs. no.:I 29.151 : 01-95.

1. Rock bursts—Congresses. 2. Mine roof control—Congresses. 3. Coal mines and mining—Safety measures—Congresses. 4. Mines and mineral resources—Safety measures—Congresses. I. Title. II. Series: Special publication (United States. Bureau of Mines); SP 01-95.

TN317.M35 1995 622'.28—dc20 95-7138 CIP